DYN-16 | 173

A.M.E.

MILITARY TECHNICAL COLLEGE

CAIRO - EGYPT

EFFECT OF PARTIAL ROTOR-TO-STATOR RUB ON SHAFT VIBRATION

Prof. Dr. S.D. Hassan*, Dr. M.R. Haddara** & M.A. Abouzaid**

ABSTRACT

The effect of partial rotor-to-stator rubbing is studied both experimentally and analytically. The measured vibration signal is distorted showing a flattenned portion of the waveform. Spectral analysis indicated that light rubbing induced vibration is characterized by harmonics at frequencies equal to 1/rev., 2/rev. and 3/rev. Severe rubbing is identified by a spectrum containing subharmonics at 1/3, 2/3 of the rotational frequency. The synchronous component is generally attenuated as a result of rubbing introduced friction. Because of the stiffening effect of rubbing on the rotor, the resonance frequency is further delayed. The results obtained analytically show good qualitative agreement with the experimentally obtained ones.

INTRODUCTION

Rubs are typically introduced by contact between the rotating and the stationary elements of a machine. Preserving ample clearances prevents rubbing from becoming a serious problem. However, very often a shaft is bent or lateral vibrations of a rotor become excessive. This results in a reduction of clearances and as a consequence rubbing takes place.

Two extreme cases of rotor rubs may be mentioned. Full annular rub happens when the rotor maintains contact with a stator (e.g. a seal), during the complete revolution, and partial rub when the contact occurs during a portion of the period of precession. Another type of rub deserves mention is the so called drywhirl. In this case the rotor just rolls around inside the stator clearance like a planetery gear with an enormously high frequency. This can happen for example when inducer vanes of open impellers radially strike the stationary shround if

* Cairo University - Faculty of engineering.

** Kuwait institute of technology.

rotor flexibility allows this type of orbiting.

Full rub is normally preceded by partial rub. With partial rub onset the rub point begins to act as a new dry nonlubricated bearing supporting the rotor. This new bearing introduces new physical phenomena as it substantially modifies the dynamic characteristics of the system. The modifications are briefly an increase in the average spring constant of the rotor and introduction of friction forces as a result of the relative motion between the stator and the rubbing rotor.

Vibrations generated by the running mechanism are very complex in nature and may lead to a total destruction of the machine in just few rotations. The rub related vibrations in turbomachinery have been documented in several publications 1 - 7. As was observed by published researches, the partial rotor/stator rub often causes a steady subharmonic at a frequency of half of the rotational speed. Experimental work performed to examine the subsynchronous frequency resulting from rotor rub indicated that the half speed motion is the general result of a rotor running at a speed equal to twice its natural frequency. Bently 1 interpretted his experimental findings in terms of analytical results using linear parametric excitation phenomena modeled by Mathieu equation.

In another published work dealing with non-synchronous clearance effects Ehrich and Oconnor 2 employed non linear simultations to explain the ½ frequency field data. Ehrich 3 employed nonlinear analysis and simulations to explain the sum and difference frequency phenomena, reported by his experimental investigations. Both rotor units examined by Ehrich were supported by roller bearings.

Childs 4,5 carried out an analysis based on Jeffcott model. He provided a linear parametric explanation for the ½ speed frequency response results obtained by Bently's rub condition. The analysis explained ½ speed wihirling motion occurring in rotors which are subjected to rub caused by radial stiffness variation. His linear parametric analysis demonstrates that during rubbing condition, coloumb damping significantly widens the potential range of unstable speed.

Musznska 6 described the physical phenomenon related to rotor rub. Rotor response shows the existance of steady state subharmonic vibrations of the order of ½, 1/3, 1/4 as a result of rotor transient free lateral vibrations.

The purpose of this work is to carry out experimental and mathematical analyses in order to gain experience with diagnostics of rotor-stator rub condition. A setup is built to carry out experiments on a rotor bearing system. The experimental observations are used to propose a mathematical model for rub identification. The analysis provides few modifications to the mathematical models of the problem worked out by childs and

with the rotor housing is introduced in terms of a nonlinear function added to the equation of motion. Similarly the frictional force developed as a result of the relative motion between rubbing elements, is expressed in a nonlinear form. Unlike Beatty's model 7 , which assumed a rigid casing, the housing in the present analysis is treated as a flexible member.

I. EXPERIMENTAL WORK

A. TEST RIG

The rig shown in figure (1) is used to study the problem. The rig consists of a heavy disc mounted centrally on a steel shaft having a young's Modulus of 207×10^5 MN/m^2. The disc has a diameter of 0.070 m. The shaft has a uniform diameter of 0.018 m. Two antifriction ball bearings are used to support the shaft. The span between the bearings is 540 mellimeters.

The rotor is driven by a D.C. motor capable of running the system up to 6000 rpm. The rotor is connected to the motor through a steel spring which acts as a flexible coupling. Four rubber mounts are used to isolate the vibration generated by the system from being transmitted to the foundation.

To carry out rub experiments a cantilever angle made of brass is bolted to the rotor casing. By controlling the clearance between the brass angle and the rotor, different conditions of rubbing are created.

Vibration measurements for the stationary component are obtained using an electrodynamic velocity pickup. The absolute velocity sensed by the pickup is integrated to obtain the absolute displacement. Shaft vibration measurements relative to the base are collecred using a noncontact eddy current proximity probe. Rime domain signals are displayed on a two channel oscilloscope. The outer circumference of the rotor is divided into 36 equal divisions so that angular location of unbalance present in the rotor is determined. The quartz controlled frequency generator and the high intensity strobe lamp on the analyzer make it possible to measure unbalance angular location and the shaft rotational speed as well. A block diagram of the experiment setup is shown in Fig.(2).

B. EXPERIMENTAL RESULTS

To investigate fully the rubbing induced forces and their effect on rotor vibrations, two sets of experiments were run. First, vibration measurements were obtained for the no rub case. These measurements were used to estimate the rotor dynamic characteristics. Second, the brassangle was put in place, and measurements were carried out for the rub condition. In the following both cases are described and discussed.

B . 1) NO RUB CONDITION

Vibration measurements of the shaft in terms of P-P displacement are obtained at different speeds. A non-contact is located horizontally 40 mm away from the midspan rotor. The probe is attached to the base of the rig where the bearing blocks and the driving motor are directly mounted.

Results from baseline are presented in figure 4 through 12. Figure 4 shows the probe output at speed 2800 rev/min. Frequency analysis of this time base signal is shown in Figure 4.b.

Figure (5) represents the sychronous horizontal response of the rotor as a function of speed. The variation of phase angle with speed is also plotted. The critical speed of the shaft is defined by the large peak amplitude observed at speed 4100 rpm, associated with a phase shift of 90^{o}. As the critical speed is passed the amplitude of vibration decreases and 180 degrees phase shaft is detected.

Bearing vibrations are measured in terms of displacement using a velocity pickup. Figures (6) and (6.b) represent the bearing vibrations in both time and frequency domains at a running speed of 3000 rpm.

The experimental data described above indicate that the unbalance present in the system is the source of these vibrations. This is varified by the sinusoidal shape of time base recorded signals as well as the sychronous response shown by spectral analyses of these signals.

B. 2) OPERATION WITH RUB ONSET

The osilloscope picture shown in figure (7) is taken while rubbing is applied to the system. The shaft rotational speed is 1500 rpm. The flat portion observed in the signal is a consequence of rub' onset. The duration time of this flat portion is a direct measure of the rubbing arc. In addition, the angular location of the rubbing element referred to the position of the measuring problem can also predicted. The spectrum shown in Figure (7.b) indicates the presence of harmonic frequency components up to the forth harmonic. It is noticed that the third harmonic is larger than both the second and the forth.

Shaft vibrations at a speed of 2400 rpm is shown in figures (8) and (8.b) respectively. The waveform characterized by the flattened shape is still detected. The spectral analysis of this signal presented in Figure (8.b) shows increased magnitude of frequency components. Figure (9) is another Oscilloscopic picture of rotor vibration taken at relatively high speed, (3900 rpm). The resulting motion is steady and periodic. The spectral analysis shows a reduction in the magnitude of the second harmonic and the disappearance of higher frequency

6

the contact arc increased as the rotor speed is increased. This is associated with a decrease in the average angular variation of rotor stiffness due to contact with the stator. Should the rubbing angle ultimately approach 360 degrees, the average rotor stiffness variation is brought to zero.

Figure 10.b is a frequency spectrum registered at a rotational frequency of 4400 rpm. The bandwidth of the analyzer is selected at 150 rpm for fast recording. It was believed that a great deal of high frequency vibration activity is included. Details of these vibrations were examined by shifting the band selector to the 45 rpm bandwidth. The resulting spectrum contains subsynchronous vibration at 1/3, 2/3, of the rotational frequency. Subsynchronous vibrations is also observed at speed equal to 4400 rpm. In addition, it is noticed that at high speeds, rubbing induced vibrations are not identified by a single frequency component but are rather distributed over a relatively broad bands centralized by the synchronous frequency and its multiples.

Two probable factors could lead to the appearance of vibration bands. The first is the friction forces which are of course a consequence of applied rubbing. These friction forces apply a frictional torque opposing the rotor motion, resulting in a fluctuation of rotor speed. So that the frequency spectrum would contain vibration component corresponding to these modified precessional speeds. On the other hand, the transient vibration which follows the removal of the friction torque in the rub free zone, could be another reason.

Figure (11) represents the response of rotor casing to which the rubbing element is attached. The signal is detected by means of an electrodynamic velocity pickup. The pickup output is integrated with respect to time to obtain displacement response. The frequency spectrum of the signal, (Fig.11.b), shows components at unrelated frequencies. It is difficult to explain these vibrations as little is known about dynamic characteristics of the casing.

Synchronous response of the rotor measured as a function of speed is plotted in figure (12). The amplitude is measured in mils (peak-to-peak) and the phase angle is referred to vertical direction.

During the experimental procedure few unstable zones have been pointed out. These zones are bounded by speeds 2300 and 2600 rpm and 4000 - 4200 rpm. Vibration measurements in the ranges were difficult to collect as they were highly changeable. Also the rotor was running very roughly and was obviously unstable.

Rubbing seems to have a potential effect on rotor response as the amplitude of vibration is largely attenuated compared with no rub vibrations. It is also noticed that the critical speed of the rotor is farther delayed due to rubbing. The response

curve indicates that this speed is larger that 4400 rpm. It is understood that the contact between the rotor and the stator would increase the dynamic stiffness of the rotor. This increase in rotor stiffness is dynamically followed by an increase in rotor critical speed.

II. MATHEMATICAL ANALYSIS

In order to gain more insight into the vibration producing rubbing mechanism and its effect on the response of rotating machinery. The experimental investigation is complemented by an analytical approach to the problem. In the analytical approach a mathematical model is formulated, and the equations obtained are solved for the two cases of light and severe rubbing. The solution in the first case is obtained using a perturbation technqiue, while a numerical solution is used for the second case. 8,9 .

Details of the mathematical model used for the derivation of the equation of motion are depicted in figure (13). The model consists of a massless shaft having one rotor and rubbing is applied to the rotor during an angle of contact. The onset of rubbing is denoted by an angle B, from the horizontal axis.

As a result of rubbing, the rotor is acted upon by two forces, Fr and Ft as shown in Figure (13). The transverse force Fr, is caused by the effect of the stiffness of the stator amd a tangential frictional force.

The results of the analytical approach for the case of light rubbing are shown in figures (15.a, b, and c.). Harmonics are calculated for a rubbing angle equal to 0.5 and a stator to rotor stiffness ratio of 0.5. Under these specified rubbing conditions, the magnitude of the harmonics as shown by the figures are so small that they may not have a serious effect on rotor dynamics. These results imply that rubbing is not always, as reported by many authors 1 - 7 a source of instability. Rubbing under certain conditions can actually be controlled. In practice, most rubbing rotors as reported by Beatty (8) generally operate fairly well, although they may experience occasional failures. Time response and rotor precessional orbit are calculated for a speed ratio (w/wn) of 0.9. Comparing these results with no rub condition shown in figures (16.a, b.c) Peak to peak amplitude of the waveform is reduced because of rubbing induced damping. Also the normally rub free circular orbit is modified to an ellipse as a result of rub onset.

For the case of heavy rub condition the analytical approach cannot be used and one has to take recourse to numerical solutions. A fourth order Runge-Kutta technique has been used to solve the equations of motion. In this program, the step size is adjusted automatically to give a solution within present limits of accuracy.

Rotor response vibrations as a function of time is calculated at a rotor speed equal to 390 rads for different values of the rubbing angle. Size of integration step is selected as 0.00075 second and the maximum allowed error in rotor response is 0.5% of the assumed one mil shaft eccentricity. With the exception of the rubbing angle the other parameters describing the system dynamic characteristics such as critical speed, stiffness, ratio, damping coefficient and obstacle location remain unchanged.

Figures 17.a, b and c. are computer plots of rotor response versus time for three different rubbing angles. The magnitudes of these angles are 0.5, 1 and 1.5 radians respectively. These figure describe the rubbing progress from initial stage to the eventual rotor instability as the rubbing arc increases. It is clearly seen that the waveform is largely affected by contact arc length. The figures show time trace having a flat portion. This flat portion is an indication of the presence of rubbing forces in the system as indicated by experimental analysis.

The peak to peak amplitudes based on predicted response are found to be affected by rubbing duration. Friction forces due to rubbing introduce to the system a coloumb type of damping whose level is proportional to the arc during which contact is maintained. Figures (17.a, and b.) indicate that vibration amplitude dropped from 5.75 to 2.616 mils as the rubbing angle is increased from 0.5 to 1.5 radians. It should be noted the calculated amplitude for a rub force shaft (= 0) rotating at the same speed is 8.5 mils.

When thecontact arc was increased to 1.5 radians the vibration amplitude was found to sharply increase, and it was not possible to obtain a steady state solution for this particular case. Apparently the rotor reached an unstable zone of operation caused by rubbing.

Shaft orbits are obtained for two different angles of contact using the numerically calculated response in both horizontal and vertical orbits. The figures indicate that orbits are significantly distorted by introducing rubbing into the system. The banana shape orbit obtained for a rubbing angle of 0.5 is gradually modified to a semi elliptic shape should the contact angle be increased to one radian.

CONCLUSION

Reviewing the experimental ana analytical results the following conclusions are mentioned.

a) The numerically predicted waveform shows a considerable resemblence to the photographed rotor rubbing response. This resemblence is demonstrated in the flattened portion of time domain response. This is considered a significant characteristic that identifies rubs experienced by rotating machines.

b) Shaft precessing orbits are largely disorted due to rubbing. In addition the phase angles of synchronous amplitudes are greately modified. Whence both orbits and phase are major parameters to diagnose rubbing rotors.

c) Friction forces associated with rubbing introduce dry damping effect into the system. Synchronous vibration amplitudes are thus attenuated. Both the experimental measurements and mathematical results indicated such trend.

d) Spectral analysis has shown that rubbing onset may best be examined by observing super harmonics and subharmonics as well. Synchronous component proved to be misleading in this aspect.

e) Rubbing angle is a very important variable to analyze if it is required to investigate rotor instability. In the presented analysis, a rubbing angle of 90° is found to be a separation point between non-distrutive and distructive rubbing. This angle is expected to vary as system dynamic characteristics vary. A further work is required to provde data about the relation between rubbing contact angle and system parameters such as stator stiffness, rotor speed, etc.

References:-

1. Bently, D.E., Forced Subrotative speed Dynamic Action of Rotating Machinery, ASME Publication 74-Pet-16.
2. Ehrich, F.F., O' Connor, J.J., Stator Whirl with rotors in bearing clearance, ASME WA/MD-8, paper 66, 1966.
3. Ehrich, F.F., The Dynamic stability of Rotor-Stator Radial Rubs in Rotating Machinery, Paper ASME, 56, No.6, 1969.
4. Child, D.W., Rub-Induced Parametric excitation in Rotors, The University of Louisville, Kentucky, 1980.
5. Childs, D.W., Fractional-Frequency Rotor Motion Due to Non Synchronous clearance effects ASME Publications 81-Gt-145 International Gas Turbine Conference and Products Show, Hauston, Texas, March 1981.
6. Muznska, A. Partial Laterial Rotor to Stator Rubs, Vibration in Rotating Machinery, Institution of Mechanical Engineers, Sept. 1984.
7. Batty, R.F., Differentiating Rotor Response due to Radial Rubbing, Journal of Vibration Acoustics, Stress and Reliability in Design. April 1985, Vol. 107.
8. Nayfeh, A.H., Nonlinear Oscillation, A Wiley-Interscience Publication, 1979.
9. Gerald, C.F., Applied Numerical Analysis, Addision-Wesky Publishing Company - 1970.

6

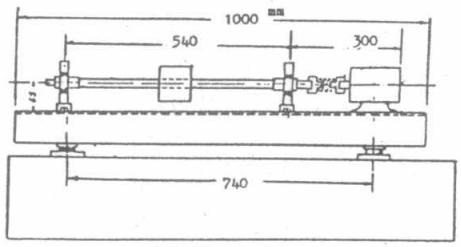

Fig. (1) Test Rig Construction

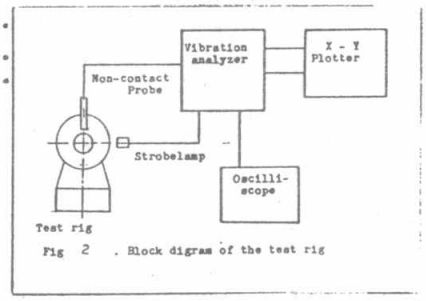

Fig 2 . Block digram of the test rig

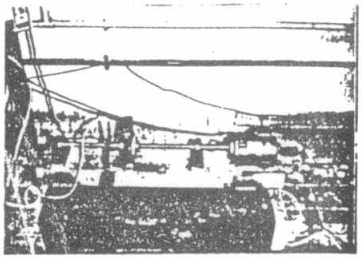

Fig 3

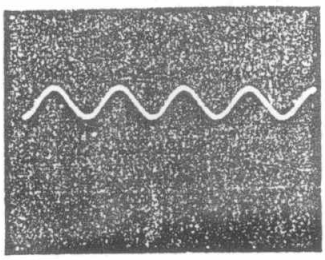

Fig. (4)
Shaft unbalance waveform Vertical response
Speed 2890 rpm

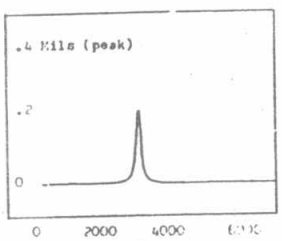

Fig.(4 -a)
Shaft unbalance response ,in the frequency domain. (speed 2890 rpm

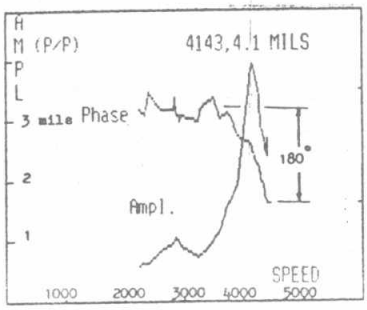

Fig 5 Response curve

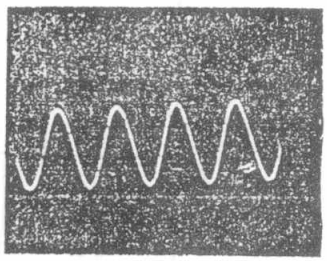

Fig. (6)
Bearing vibration waveform.
Pickup Vertical (speed = 3000 rpm)

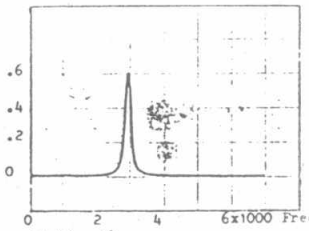

Fig(6 - b)
Spectral analysis of bearing vibrations (displacement)

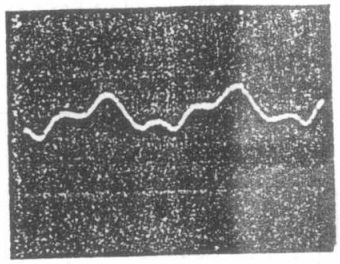

Fig.(7)
Time domain signal - Speed =1500 RPM

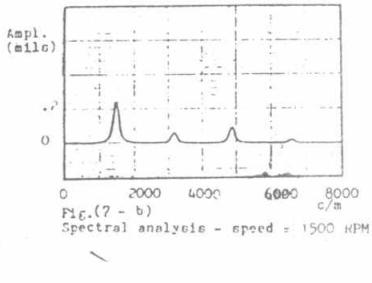

Fig.(7 - b)
Spectral analysis - speed = 1500 RPM

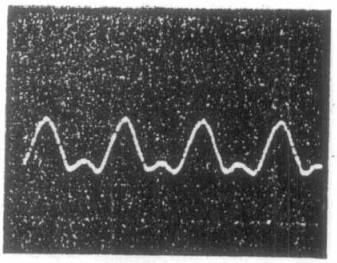

Fig. (8)
Time history photograph - Speed 2400 RPM
Under applied rubbing

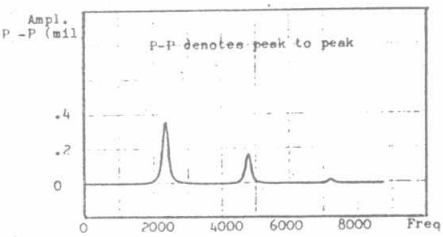

Fig. (8-b)
Spectral analysis of rubbed rotor
(speed=2400 rpm)

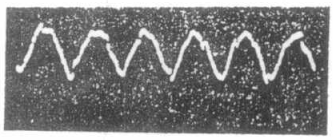

Fig. (9)
Time domain signal of shaft displacement
(speed - 3900)

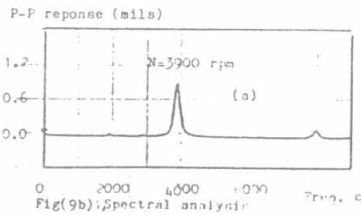

Fig(9b);Spectral analysis

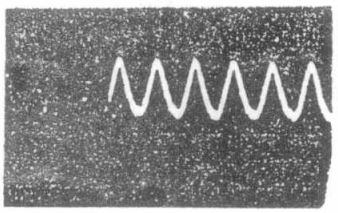

Fig. 10 Time history of shaft vibrations
Rubbing applied. - (N=4400 rpm)

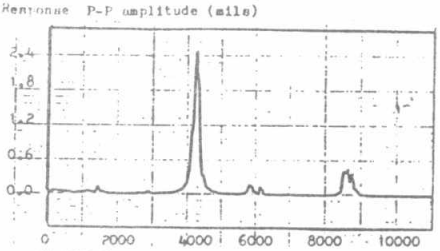

S ND A.M.E. CONFERENCE
6 - 8 May 1986 , Cairo

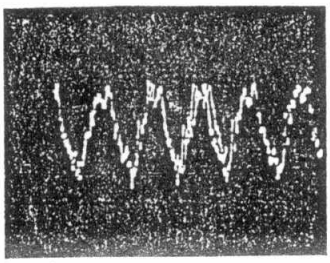

Fig 11
Response of electrodynamic velocity picku
-Probe mounted horizontally on casing
(N = 3300 rpm)

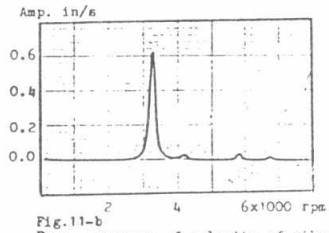

Fig.11-b
Freq. response of velocity of vibr.

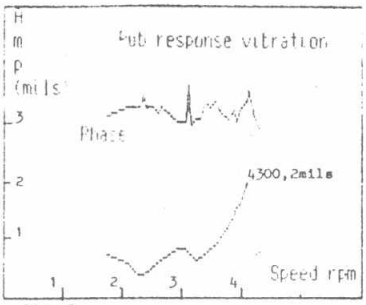

Fig.12

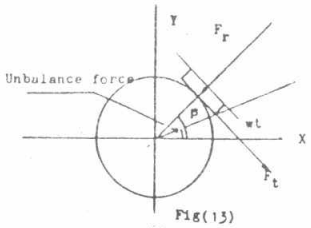

Fig(13)

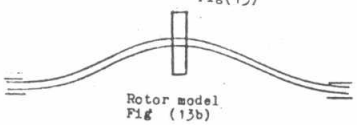

Rotor model
Fig (13b)

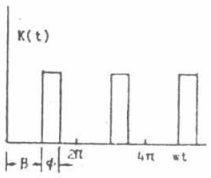

Fig.(14)

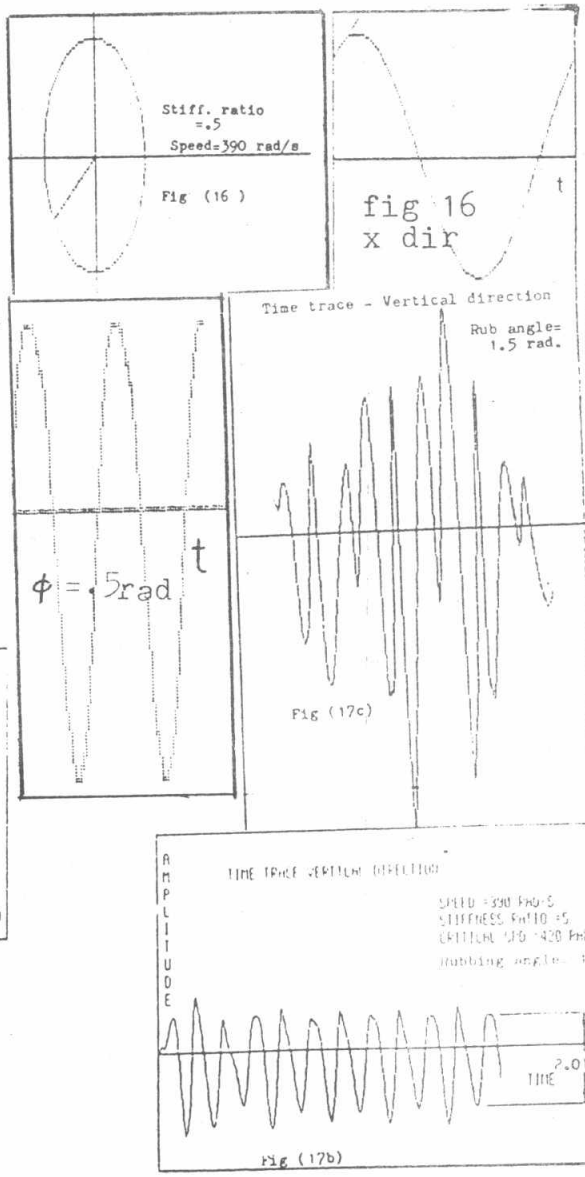

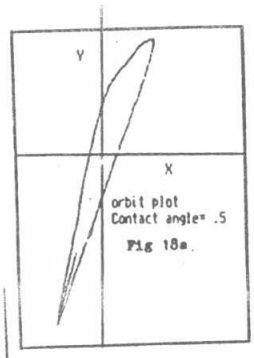

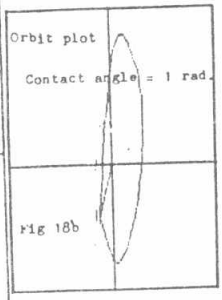

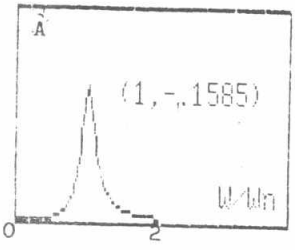

Fig15aAnalytic sol. (Sync. comp. 1st order)

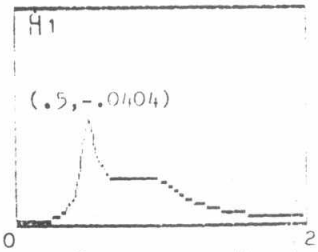

Fig 15b 2/rev amp. W/Wn

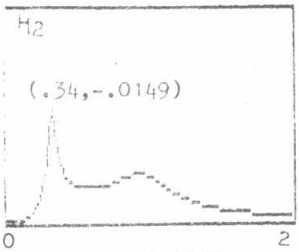

3/rev ampl.W/Wn
Fig 15c